Materials Letters 276 (2020) 128246

Contents lists available at ScienceDirect

Materials Letters

journal homepage: www.elsevier.com/locate/mlblue

Synthesis of magnetite, ceria and magnetite-ceria materials by calcination of nanostructured precursor-minerals

German Montes-Hernandez

UGA, USMB, CNRS, IRD, IFSTTAR, ISTerre, 38000 Grenoble, France

ARTICLE INFO

Article history:
Received 14 May 2020
Accepted 29 June 2020
Available online 1 July 2020

Keywords:
Magnetic materials
Composites
Crystallization
Electron microscopy

ABSTRACT

The present short communication reports an original experimental calcination method to synthesize magnetic materials with high thermal stability such as magnetite (Fe_3O_4) with typical spinel and atypical crystal shape, sub-micrometric rounded crystals of ceria (CeO_2) and magnetite-ceria composites with varied shape and size of crystals. Shape and size depending on the nature of mineral precursors (goethite, siderite or ferrihydrite). Herein, it was demonstrated that cooperative redox reactions and simple vacuum can be used to synthesize magnetic composite materials by calcination of nanostructured mineral precursors. In this way, bastnäsite mineral ($CeCO_3F$) is a powerful reducing agent to synthesize magnetite from reductive dehydration of ferric oxyhydroxides.

1. Introduction

Synthetic ceria (CeO_2) and magnetite (Fe_3O_4) are crucial oxides in many industrial and/or medical applications related to their extraordinary chemical properties (acid-base and oxidation-reduction behavior), thermal stability and oxygen mobility [1–6]. Both minerals have found their applications in catalysis (photo-), luminescent materials, fuel cell, free radical scavenger, gas sensor, cosmetic material, optical additives, polishing materials, water splitting, ceramic pigments, biomedicine, magnetic storage media, etc. [1–6]. In general, magnetite or ceria are independently used; however, recently their association as magnetite-ceria composites have been also explored in catalytic reactions, for example, in the degradation of organic molecules [7], in Fenton reactions [8], in multicomponent redox reactions [9] and in the dephosphorylation of phosphopeptides [10]. In this way, the improving of existing methods and/or developing innovative routes to obtain well-controlled crystal shapes and sizes remain important challenges in materials science. The present short communication reports an original calcination method to synthesize magnetite, ceria and magnetite-ceria composites with high thermal stability and probably with relevant catalytic properties by using dynamic vacuum ($\approx 5 \times 10^{-6}$ mbar) and bastnäsite ($CeCO_3F$) nanostructured mineral as reducing agents. In fact, four nanostructured minerals goethite (FeO(OH)), siderite ($FeCO_3$), ferrihydrite 6-lines and bastnäsite ($CeCO_3F$) were synthesized at low T (<95 °C), methods already published by my group [11–14]. Then the obtained nanostructured minerals are used as powdered precursors in order to synthesize magnetite from reductive dehydration of goethite or from oxidative decarbonation of siderite, ceria from oxidative decarbonation of bastnäsite and magnetite-ceria composites from cooperative and/or competitive redox reactions. Mineral composition and crystal shape and size were mainly determined by XRD and FESEM.

2. Materials and methods

2.1. Synthesis of mineral precursors and nano-magnetite reference

Goethite, siderite, ferrihydrite and bastnäsite minerals were synthesized by using already published methods [11–14]. In supplementary information, only the overall reaction of synthesis of precursor and magnetite reference, including a basic characterization by XRD and FESEM are provided (Fig. SI-1).

2.2. Synthesis of magnetite, ceria and magnetite-ceria composites

2.2.1. Magnetite from oxidative decarbonation of siderite

2 g of dry siderite placed in an alumina ceramic crucible were calcinated at 500 °C under secondary vacuum ($\approx 5 \times 10^{-6}$ mbar) for 5 h by using a quartz tubular reactor. A heating rate of 30 °C/min was performed in all experiments. At the end of experiment, the calcinated product were cooled under dynamic vacuum at room temperature (~19 °C).

E-mail address: german.montes-hernandez@univ-grenoble-alpes.fr

https://doi.org/10.1016/j.matlet.2020.128246
0167-577X/

2.2.2. Magnetite from reductive dehydration of goethite

1 g of dry goethite and 1 g of dry bastnäsite placed independently in an alumina ceramic crucible (e.i. without solid–solid contact) were calcinated at the same above conditions. In this case, the bastnäsite transformation into ceria (CeO_2) improves the reducing conditions in the reactor allowing complete goethite transformation into magnetite.

2.2.3. Ceria from oxidative decarbonation of bastnäsite

2 g of dry bastnäsite placed in an alumina ceramic crucible were calcinated at the same above conditions.

2.2.4. Synthesis Fe_3O_4-CeO_2 composites

Three different binary mineral-precursor mixtures (ferrihydrite-bastnäsite, goethite-bastnäsite and siderite-bastnäsite) were manually prepared by using equivalent weighs in an agate mortar and mixed by a pestle. Then, 2 g of each mineral mixture were placed in an alumina ceramic crucible and calcinated at the same above conditions.

All calcinated solid products were manually recovered and stored in plastic flasks for subsequent characterization by XRD and FESEM (see supplementary information).

3. Results and discussion

All main results are summarized in Figs. 1 to 3 concerning particularly FESEM images and XRD patterns of calcinated products. Based on this conventional solid characterization for precursors (Fig. SI-1) and calcinated products, an overall redox reaction for each investigated scenario is suggested as follows:

3.1. Magnetite formation from goethite

$$3FeOOH \Rightarrow Fe_3O_4 + 0.25O_2 + 1{\cdot}5H_2O \quad (1)$$

The formation of magnetite is improved when bastnäsite mineral is used as supplementary reducing agent in the reactor (see Fig. SI-2). In such case, the Ce(III) oxidation to Ce(IV) initially contained in cerium carbonate creates a most reducing atmosphere into the reactor during calcination process. FESEM images have revealed two crystals shapes of magnetite, typical spinel shape and acicular crystals; letter shape was probably inherited from original goethite shape (Fig. 1).

3.2. Magnetite formation from siderite decarbonation

$$3FeCO_3 + 0.5O_2 \Rightarrow Fe_3O_4 + 3CO_2 \quad (2)$$

The constrained dynamic vacuum was enough to favor the magnetite formation rather than hematite (Fe_2O_3). Assuming that water is also present in the system (residual water in vacuum atmosphere), the following oxidative reaction ($3FeCO_3 + H_2O \Rightarrow Fe_3O_4 + 3CO_2 + H_2$) could also contribute to magnetite formation. Surprisingly, synthesize magnetite have conserved the initial shape

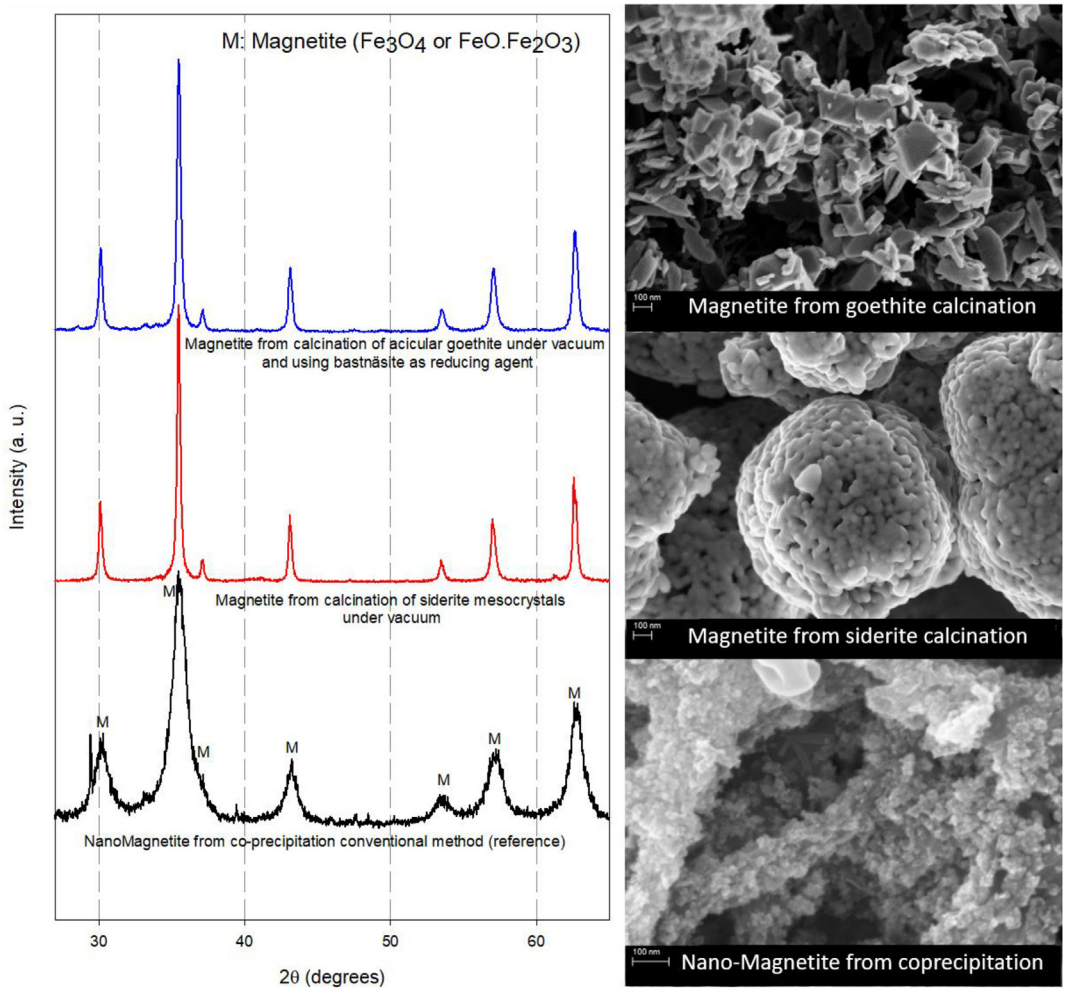

Fig. 1. XRD patterns for three magnetite synthesized for three different reaction pathways and FESEM images showing shape and size of magnetite crystals.

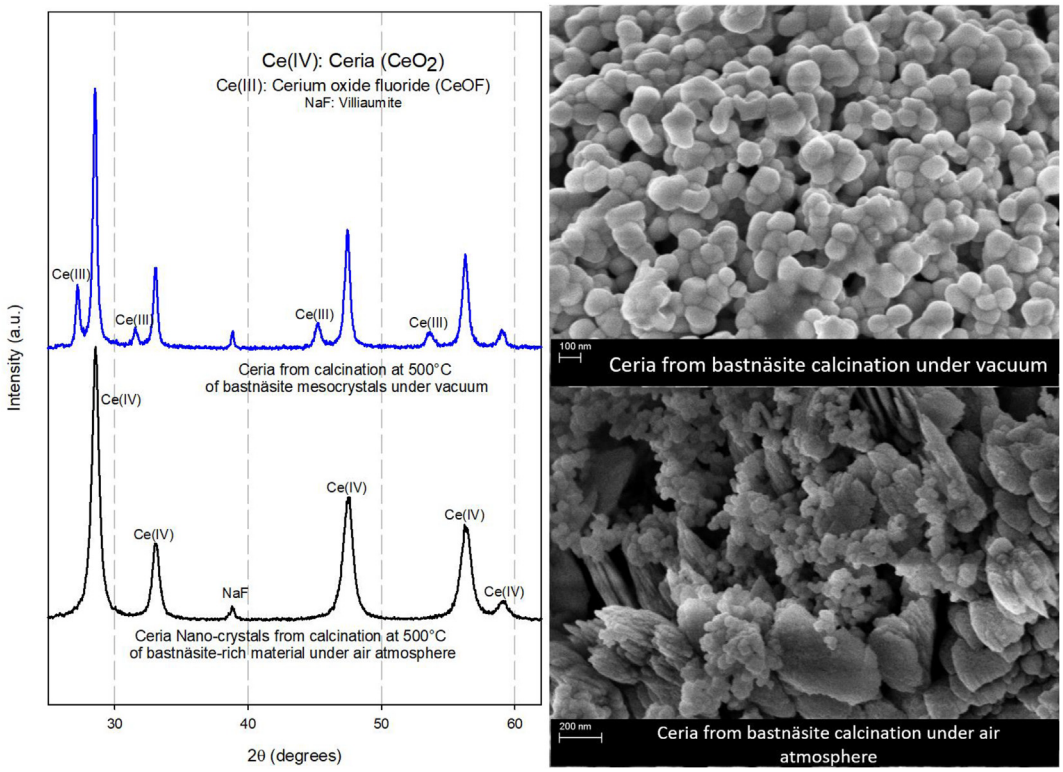

Fig. 2. XRD patterns for two ceria synthesized under air atmosphere (reference) and under dynamic vacuum and FESEM images showing shape and size of ceria crystals.

of siderite spherical aggregates as revealed by FESEM, however, the magnetite micrometric (<3μm) spherical agglomerates constituted by magnetite nanoparticles are now observed (Fig. 1).

3.3. Ceria formation from bastnäsite decarbonation

$$2CeCO_3F + O_2 \Rightarrow 2CeO_2 + 2CO_2 + F_2 \quad (3)$$

This reaction can be auto-enhanced by in situ produced flour than can react with residual water in the system to form additional oxidants (e.g. $F_2 + H_2O \Rightarrow 0.5O_2 + 2HF$). However, the XRD has also revealed cerium oxide fluoride (CeOF) that is generally a transient phase during cera formation from oxidative decarbonation of bastnäsite ($CeCO_3F \Rightarrow CeOF + CO_2$) with a short lifetime under air atmosphere as already demonstrated [12]. Finally, FESEM images have revealed rounded ceria nanoparticles with high agglomeration degree with respect to ceria formed under air atmosphere (see Fig. 2).

3.4. Magnetite-Ceria composite from ferrihydrite-bastnäsite mixture

$$3Fe_2O_3.2(FeO(OH)).nH_2O \Rightarrow 4Fe_3O_4 + O_2 + (n + 3)H_2O \quad (4a)$$

$$2CeCO_3F + O_2 \Rightarrow 2CeO_2 + 2CO_2 + F_2 \quad (4b)$$

A complete transformation of ferrihydrite into magnetite was particularly possible by means of cerium oxidation contained in bastnaesite. This means that a cooperative double-redox reaction exists: Fe^{3+}/Fe^{2+} and O^{2-}/O_2 for magnetite formation and Ce^{3+}/Ce^{4+}, O_2/O^{2-} and F^-/F_2 for ceria formation. In terms of mineral composition, the XRD has revealed magnetite and ceria as major phases and a minor proportion of cerium oxide fluoride (CeOF) and sodium fluoride (NaF) were also detected in final products, indicating an incomplete oxidation of cerium initially contained in bastnäsite mesocrystals (see XRD patterns in Fig. 3). FESEM images have revealed homogeneous mixture of micrometer magnetite crystal (<2μm) with spinel shape and sub-micrometric ceria crystals with rounded shape. Ceria particles adhered onto magnetite crystals or forming aggregates.

3.5. Magnetite-Ceria composite from goethite-bastnäsite mixture

$$3FeOOH \Rightarrow Fe_3O_4 + 0.25O_2 + 1{\cdot}5H_2O \quad (5a)$$

$$2CeCO_3F + O_2 \Rightarrow 2CeO_2 + 2CO_2 + F_2 \quad (5b)$$

This cooperative double redox reaction is identical to ferrihydrite-bastnäsite system, however, different crystal shape and size and different water content exist between goethite and ferrihydrite (see Fig. SI-1). As expected, magnetite-ceria composite was synthesized as revealed from XRD patterns. In this case, sub-micrometric magnetite crystals with spinel shape are homogeneously mixed with nanometric ceria rounded-crystals having high agglomeration and/or aggregation degree as observed in the FESEM image (Fig. 3).

3.6. Magnetite-Ceria composite from siderite-bastnäsite mixture

$$3FeCO_3 + 0.5O_2 \Rightarrow Fe_3O_4 + 3CO_2 \quad (6a)$$

$$2CeCO_3F + O_2 \Rightarrow 2CeO_2 + 2CO_2 + F_2 \quad (6b)$$

Contrary to two above cooperative redox systems, here, an oxidative-decarbonation competition exists as illustrated in reactions (6a) and (6b). Despite this competition, the magnetite-ceria composite was successfully synthesized as revealed by XRD (Fig. 3). However, a more reducing environment in the reactor was created because a higher proportion of cerium oxide fluoride (CeOF)

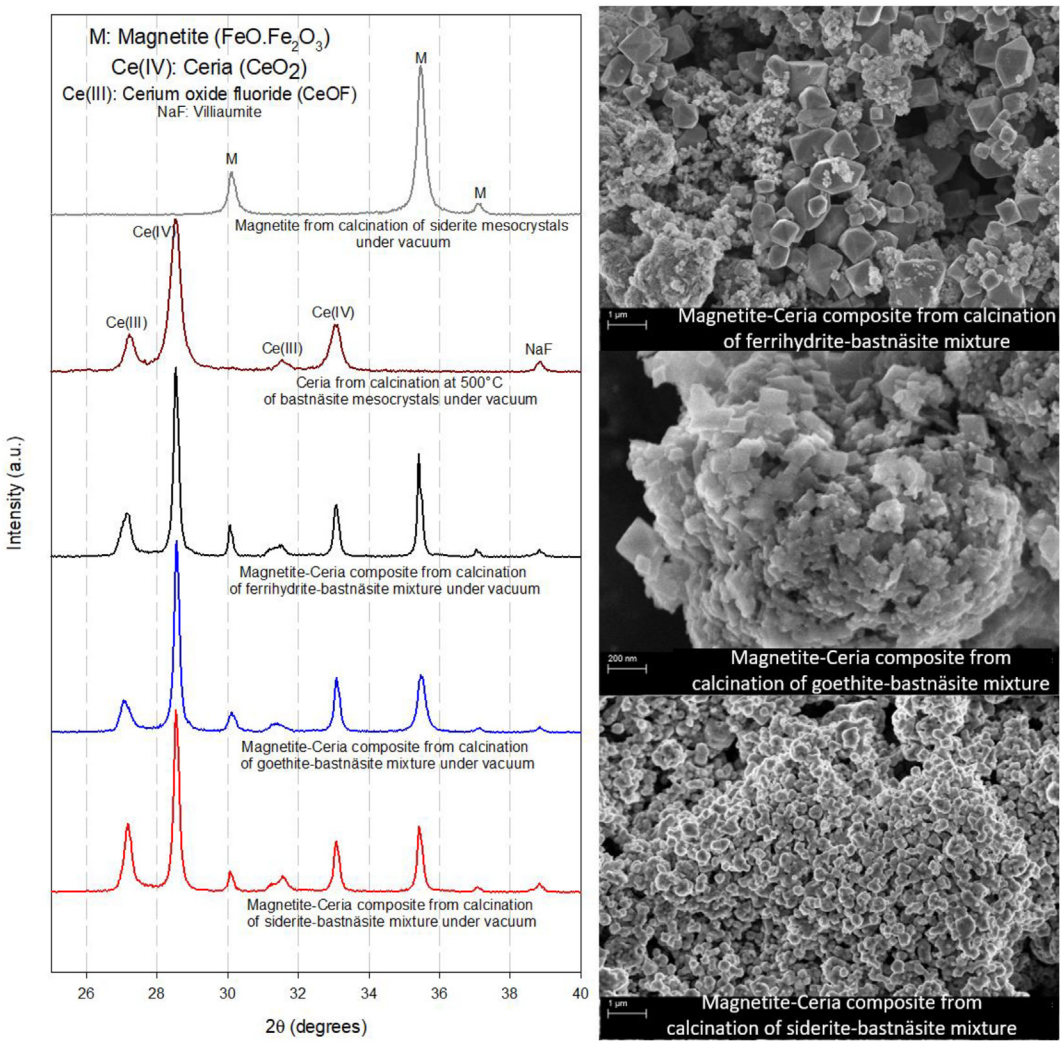

Fig. 3. XRD patterns for three magnetite-ceria composite materials synthesized by calcination of three different mineral-precursor mixtures and FESEM images showing shape and size of magnetite crystals.

and also iron oxide (FeO) were detected; both mineral phases implying only decarbonation process without oxidation, possible only in high reducing systems. FESEM images have revealed submicrometric magnetite and ceria crystals with rounded shape and with high agglomeration degree (see Fig. 3 and Fig. SI-3).

4. Conclusion

Magnetite with typical spinel and atypical crystal shape, submicrometric rounded crystals of ceria and magnetite-ceria composites with varied shape and size of crystals were synthesized by calcination under dynamic secondary vacuum and using bastnäsite as complementary solid reducing agent.

Declaration of Competing Interest

The authors declare that they have no known competing financial interests or personal relationships that could have appeared to influence the work reported in this paper.

Acknowledgements

The authors are grateful to CNRS and UGA for providing funding support. IPAG is grateful for allowing the access to calcination experiments. We thank Nathaniel Findling, Olivier Brissaud, Pierre Beck and Eric Quirico for their technical assistance.

Appendix A. Supplementary data

Supplementary data to this article can be found online at https://doi.org/10.1016/j.matlet.2020.128246.

References

[1] A. Bumajdad, J. Eastoe, A. Mathew, Cerium oxide nanoparticles prepared in self-assembled systems, Adv. Colloid Interface Sci. 147–148 (2009) 56–66.
[2] E. Leino, P. Maki-Arvela, V. Eta, N. Kumar, F. Demoisson, A. Samikannu, A.R. Leino, A. Shchukarev, D.Y. Murzin, J.P. Mikkola, The influence of various synthesis methods on the catalytic activity of cerium oxide in one-pot synthesis of diethyl carbonate starting from CO2, ethanol and butylene oxide, Catal. Today 210 (2013) 47–54.
[3] N. Gokon, S. Sagawa, T. Kodoma, Comparative study of activity of cerium oxide at thermal reduction temperatures of 1300–1550 °C for solar thermochemical two-step water-splitting cycle, Int. J. Hydrogen Energy 38 (2013) 14402–14414.
[4] J. Mosayebi, M. Kiyasatfar, S. Laurent, Synthesis, functionalization, and design of magnetic nanoparticles for theranostic applications, Adv. Healthcare Mater. (2017), 1700306.
[5] M. Usman, J.M. Byrne, A. Chaudhary, S. Orsetti, K. Hanna, C. Ruby, A. Kappler, S. B. Haderlein, Magnetite and green Rust: synthesis, properties, and environmental applications of mixed-valent iron minerals, Chem. Rev. 118 (2018) 3251–3304.

[6] J. Jolivet, C. Chanéac, E. Tronc, Iron oxide chemistry. From molecular clusters to extended solid networks, Chem. Commun. (2004) 481–487.
[7] G. Gan, P. Zhao, X. Zhang, J. Liu, J. Liu, C. Zhang, X. Hou, Degradation of Pantoprazole in aqueous solution using magnetic nanoscaled Fe3O4/CeO2 composite: effect of system parameters and degradation pathway, J. Alloy. Compd. 725 (2017) 472–483.
[8] L. Xu, J. Wang, Magnetic nanoscaled Fe3O4/CeO2 composite as an efficient fenton-like heterogeneous catalyst for degradation of 4-chlorophenol, Environ. Sci. Technol. 46 (2012) 10145–10153.
[9] M.B. Gawande, V.D.B. Bonifácio, R.S. Varma, I.D. Nogueira, N. Bundaleski, C.A.A. Ghumman, O.M.N.D. Teodoro, P.S. Branco, Magnetically recyclable magnetite–ceria (Nanocat-Fe-Ce) nanocatalyst – applications in multicomponent reactions under benign conditions, Green Chem. 15 (2013) 1226–1231.
[10] Q. Min, S. Li, X. Chen, E.S. Abdel-Halim, L.-P. Jiang, J.-J. Zhu, Magnetite/ceria-codecorated titanoniobate nanosheet: A 2D catalytic nanoprobe for efficient enrichment and programmed dephosphorylation of phosphopeptides, ACS Appl. Mater. Interfaces 7 (2015) 9563–9572.
[11] S. Hajji, G. Montes-Hernandez, G. Sarret, A. Tordo, G. Morin, G. Ona-Nguema, S. Bureau, T. Turki, M. Nzoughi, Arsenite and chromate sequestration onto ferrihydrite, siderite and goethite nanostructured minerals: Isotherms from flow-through reactor experiments and XAS measurements, J. Hazard. Mater. 362 (2019) 358–367.
[12] G. Montes-Hernandez, R. Chiriac, N. Findling, F. Toche, F. Renard, Synthesis of ceria (CeO_2 and CeO_{2-x}) nanoparticles via decarbonation and Ce(III) oxydation of synthetic bastnäsite (CeCO3F, Mater. Chem. Phys. 172 (2016) 202–210.
[13] G. Montes-Hernandez, P. Beck, F. Renard, E. Quirico, B. Lanson, R. Chiriac, N. Findling, Fast precipitation of acicular goethite from ferric hydroxide gel under moderate temperature (30 and 70 C degrees), Cryst. Growth Des. 11 (2011) 2264–2272.
[14] G. Montes-Hernandez, F. Renard, Time-resolved in situ Raman spectroscopy of the nucleation and growth of siderite, magnesite and calcite and their precursors, Cryst. Growth Des. 16 (2016) 7218–7230.